ADVANCED MATERIALS
www.advmat.de

Flexible and Stretchable Antennas for Biointegrated Electronics

*Zhaoqian Xie, Raudel Avila, Yonggang Huang, and John A. Rogers**

Combined advances in material science, mechanical engineering, and electrical engineering form the foundations of thin, soft electronic/optoelectronic platforms that have unique capabilities in wireless monitoring and control of various biological processes in cells, tissues, and organs. Miniaturized, stretchable antennas represent an essential link between such devices and external systems for control, power delivery, data processing, and/or communication. Applications typically involve a demanding set of considerations in performance, size, and stretchability. Some of the most effective strategies rely on unusual materials such as liquid metals, nanowires, and woven textiles or on optimally configured 2D/3D structures such as serpentines and helical coils of conventional materials. In the best cases, the performance metrics of small, stretchable, radio frequency (RF) antennas realized using these strategies compare favorably to those of traditional devices. Examples range from dipole, monopole, and patch antennas for far-field RF operation, to magnetic loop antennas for near-field communication (NFC), where the key parameters include operating frequency, *Q* factor, radiation pattern, and reflection coefficient S_{11} across a range of mechanical deformations and cyclic loads. Despite significant progress over the last several years, many challenges and associated research opportunities remain in the development of high-efficiency antennas for biointegrated electronic/optoelectronic systems.

1. Introduction

Some of the most compelling opportunities in biointegrated electronic/optoelectronic devices are in wireless, skin-mounted, accurate tools for collection, and transmission of biological signals related to physiological health status. The most advanced of such systems offer clinical quality data, with the capacity to operate in a continuous fashion, over long periods of time outside of clinics, hospitals, and laboratories.[1] Examples include microfluidic devices for capture and biomarker analysis of sweat,[2–6] mechanoacoustic sensors for cardiovascular diagnostics,[7,8] multinode platforms for full-body pressure/temperature monitoring,[9] technologies for characterizing the skin,[10,11] and its hydration state,[12] miniaturized pulse oximeters,[13,14] UV dosimeters,[15–17] and others. Related systems also have utility in biological research, from conformal sheets of electronics for mapping electrophysiological processes of the brain and the heart[11,18] to thin filamentary probes for optogenetic control and optical monitoring of neural activity.[19–22] The processes for wirelessly transmitting and receiving data/power to and from external devices most typically rely on integrated antennas on soft elastomers.[23–27] The electromagnetic performance depends on the geometry, and orientation for reconfigurable antennas,[28,29] the constituent materials, the surrounding environment and the mechanical responses to applied loads. The design goals center around maximizing the stretchability and minimizing the sizes, while maintaining excellent performance and performance stability.[30–34]

In radio-frequency engineering, an antenna acts as either a transmitter or receiver to link electromagnetic waves traveling through space to electrical currents in the conductive components.[35] The radiation pattern defines the strength of the radiated power as a function of the direction away from the antenna, to highlight the major/minor radiation peaks, and to reveal the efficiency. The directivity (i.e., preferred radiation direction) of an antenna describes the power received in its peak direction. A high directivity implies that the antenna is more likely to receive signals from a specific direction. For an isotropic antenna, the radiation pattern is equal in all directions, with zero directionality, corresponding to a directivity of 1 (or 0 dB). The ratio of the power delivered to and radiated from an antenna is known as the antenna efficiency. In the transmission process, the power can be radiated, absorbed as losses within the antenna, or reflected away due to an impedance mismatch with the transmission line. A high-efficiency antenna radiates most of the power and a low-efficiency antenna either absorbs or reflects the power causing poor transmission. The ratio of power transmitted in the preferred direction to that of an isotropic antenna is described as the antenna

Dr. Z. Xie, R. Avila, Prof. Y. Huang
Departments of Civil and Environmental Engineering
Mechanical Engineering, and Materials Science and Engineering
Center for Bio-Integrated Electronics, Northwestern University
Evanston, IL 60208, USA
Prof. J. A. Rogers
Department of Materials Science and Engineering
Biomedical Engineering
Neurological Surgery, Chemistry, Mechanical Engineering
Electrical Engineering and Computer Science
Simpson Querrey Institute and Feinberg Medical School
Center for Bio-Integrated Electronics
Northwestern University
Evanston, IL 60208, USA
E-mail: jrogers@northwestern.edu
The ORCID identification number(s) for the author(s) of this article can be found under https://doi.org/10.1002/adma.201902767.

DOI: 10.1002/adma.201902767

gain, expressed in decibels (dB). As one of the key parameters in antennas, the gain combines the directivity and the losses accounted in the efficiency to define the electromagnetic performance. The reflection coefficient (S_{11}), quantifies the ratio, in dB, of the electromagnetic wave that is reflected by an impedance discontinuity in the transmission medium. The bandwidth, another fundamental antenna parameter, describes the range of frequencies over which the antenna can properly radiate or receive energy (threshold limit $S_{11} < -10$ dB).[36] In the operating bandwidth of the antenna, the reflection coefficient is small, as most of the electromagnetic wave is radiated rather than reflected (assuming no losses).[35] The quality factor, or Q factor, is the quotient between the stored and radiated energies. For inductive antennas, the Q factor increases linearly with the frequency and it can be expressed as the ratio of the inductive reactance over the resistance. A high Q factor resembles the behavior of a perfect inductor.

To ensure that flexible and stretchable antennas' function properly, the effect of large mechanical deformations on the radiation properties must be considered. Deformations can degrade the antenna performance by changing the resonant frequency, bandwidth, and Q factor. This review focuses on widely used fabrication methods/materials to create the conductive components for the radiation parts in flexible and stretchable antennas. Fabrication strategies and materials for stretchable antennas span a wide range. Structures that exploit 2D filamentary serpentines and 3D helical architectures offer high levels of flexibility and stretchability when integrated with soft elastomeric substrates and/or superstrates, thereby affording the ability to integrate with the soft, time-dynamic surfaces of living organisms.[37,38] Specifically, optimized serpentine structures patterned from conventional metals offer both high electrical conductivity ($\approx 4 \times 10^5$ S cm^{-1}) and stretchability (≈300%), with reversible elastic responses without plastic yielding or fracture.[39] For the types of highly complex serpentines and mesh interconnects that are often required in practical systems, the overall strechability at the device level decreases to 20–50%.[40]

Another option in antennas relies on textiles that incorporate conductive threads embroidered in fabric to create wearable devices that support stretchable and other interesting mechanical properties.[41] The density of these threads is the main parameter that determines the conductivity and performance. A typical silver-plated copper thread has a high conductivity (≈ 1 to 5×10^6 S cm^{-1}) depending on the density, measured in ppi, or pick/threads per inch.[42] Textile systems of this type require careful control to overcome the limited accuracy, reproducibility, and quality of conventional knitted and weaved patterns, particularly when scaled to large areas.[43] Reducing the thicknesses of substrates that separate textile antennas from corresponding ground planes can improve the antenna dimensions due to an increase in the relative permittivity of the dielectric.[44] Most of the applications of textiles center on smart clothing systems.[44–47]

A third approach focuses on antennas constructed with liquid metals' exploit soft microfluidic networks, where large strains induce physical flow.[48] Low toxicity, good conductivity ($\approx 3 \times 10^4$ S cm^{-1}), and compatibility with simple patterning techniques create interest in these systems.[49] Furthermore, the self-healing characteristics of elastomeric chambers filled with liquid metals facilitate mechanically robust responses to large strains,[50–52] where discontinuities in the metal associated with microchannel collapse under extreme deformations represent the main failure mode.

Conductive nanomaterials at loading levels that exceed the percolation threshold support excellent electrical properties

Zhaoqian Xie is a postdoctoral fellow in the department of civil and environmental engineering at the Northwestern University in USA. He received his Ph.D. degree from Dalian University of Technology in China. His research interests include solid mechanics, experimental mechanics, and wireless communication/energy harvesting of wearable and biointegrated electronics.

Raudel Avila is a Ph.D. candidate in mechanical engineering at the Northwestern University. He received a B.S. in mechanical engineering from the University of Texas at El Paso. His current research focuses on the mechanics and electromagnetics of biointegrated electronics for health monitoring applications. He is a National Science Foundation GRFP Fellow and a Ford Foundation Predoctoral Fellow.

John A. Rogers is the Louis Simpson and Kimberly Querrey Professor in Materials Science and Engineering, Biomedical Engineering, Mechanical Engineering, Electrical Engineering and Computer Science, Chemistry, and Neurological Surgery at the Northwestern University where he also serves as Director of the Center on Bio-Integrated Electronics. His research focuses on unusual electronic and photonic devices, with an emphasis on biointegrated and bioinspired systems. He is a member of the National Academy of Engineering, the National Academy of Sciences and the American Academy of Arts and Sciences.

when integrated into soft stretchable matrices,[53,54] as another route to stretchable antenna designs. Carbon nanotubes (CNTs), silver nanowires (AgNWs), and graphene, each combined with an elastomer such as polydimethylsiloxane (PDMS), represent well-studied examples.[55–58] AgNWs on the surfaces of such elastomers offer excellent electrical performance for uniaxial strains <20%,[59] with significant improvements (up to 50%) when embedded just below the surface.[60] Combinations of different types of nanomaterials can lead to further enhancements. For example, AgNW/CNT hybrid structures show improved conductivity and overcome limitations in stretchability associated with pure AgNWs. Specifically, AgNW/CNTs transferred on silicone substrates at prestrains of ≈150% offer electrical stability at strains up to 460% with resistances that are smaller (≈75% smaller) that those achieved with only AgNWs.[61] Similarly, transparent graphene/AgNW hybrid structures can accommodate large uniaxial strains (≈100%) without significant changes in resistance.[62] Conductivities of nanomaterial-enabled stretchable conductors range from 440 S cm^{-1} for CNT fibers to 8130 S cm^{-1} for AgNW/PDMS.[60,63]

Electromagnetic designs can effectively improve the radiation coverage and efficiency. Strategies to enhance the radiation performance and efficiency involve truncating the ground plane to achieve a compact size with expanded radiation coverage,[64] using metasurfaces to compensate out-of-phase radiation,[65] modifying the antenna strip designs,[66] and numerical optimizing the layouts,[67] among others. These electromagnetic design strategies can be specifically applied to flexible and stretchable antennas to improve its performance upon mechanical deformation.

This review highlights key structural design, material aspects, and performance attributes of the broad classes of antennas in biointegrated or wearable electronics. Following an overview of the strategies used for fabrication, the content focuses on the performance of different types of antennas already used in wearable/skin-integrated technologies or with a strong potential to be exploited in such applications. A concluding section summarizes the future perspectives and challenges associated with miniaturization, energy management, and stable operation for future applications.

2. Antennas Based on Metal–Serpentine Structures

The development of soft, biointegrated technology platforms depends critically on enabling materials for ultrathin, ultralow modulus devices that can undergo large mechanical deformations.[68] A widely used design strategy involves thin, filamentary serpentine structures as interconnects and/or supporting platforms for electronic elements that embed within thin, soft elastomeric films,[37,38,69,70] as a type of composite material structure that combines the electrical properties of inorganic electronic systems with the mechanical properties of elastomeric polymers. In optimized layouts, these systems allow stretching, bending, and twisting deformations for seamless, conformal integration onto curvilinear surfaces of soft biological tissues, while maintaining high-performance operation. The design aspects of serpentine structures can be tailored to match the mechanical properties, including the full J-shaped stress/strain responses, of broad classes of biological tissues.[71–74] These same concepts can be naturally applied to the design of the flexible and stretchable antennas.

Kim et al. introduced layouts for near-field communication (NFC) antennas (high frequency, HF) that incorporate stretchable serpentine structures for skin-like, or "epidermal," electronic devices configured to collect and transmit data/power when mounted on the skin.[37] **Figure 1**a (left) shows such an antenna, where a low-modulus acrylic adhesive (17 kPa) with a thickness of ≈25 µm serves as the substrate.[40] This thin, soft construction allows conformal contact with the skin via van der Waals interactions alone. The antenna can operate effectively during extreme deformations associated with pinching and buckling of the skin, in a manner that also allows freedom of movement of the skin, without any apparent constraint as shown in Figure 1a (middle). Figure 1a (right) highlights the minimal shifts in operating frequency (0.3 MHz) for this type of antenna under uniaxial strains of up to ≈30%. An example application of these design concepts is in a recently reported class of wireless, battery-free, epidermal electronic system for vital signs monitoring in the neonatal intensive care unit, shown in Figure 1b. Here, although conventional NFC protocols support only simple communication operations,[75] several modifications allow high-speed, high-fidelity data transfer rates for clinical grade data acquisition.[76] Reliable communication and power transmission occur for uniaxial strains of up to ≈16%.[76] Even for 20% stretching, the Q factor, S_{11}, and resonant frequency remain largely unchanged. An additional feature that the system designs is such that the resonant frequencies avoid overlap with the working frequencies of medical resonance imaging (MRI) scanners commonly used in neonatal intensive care units (NICUs), as shown in Figure 1b (right). The result is that imaging can be performed without removing the device.

In addition to operation with NFC protocols in the HF regime, antennas for the ultrahigh frequency (UHF) band is also possible. As illustrated in the image of Figure 1c, a patch antenna with serpentine structures can serve as part of an implantable, soft wireless optoelectronic system.[77] Here, the small size allows power harvesting at frequencies between 1 and 3 GHz, as an implantable, wirelessly controlled light source for optogenetics studies on small animal models such as mice. The bandwidth at the center frequency (200 MHz) allows harvesting across a broader range of transmitting frequencies than that associated with the conventional bandwidth (50 MHz) of a patch antenna. The result provides operational robustness for a range of dielectric environments and states of deformation.[77] Uniaxial strain reduces the resonant frequency as the overall length of the antenna increases, but with minimal effect in the efficiency because the gaps between the serpentines simultaneously contract and expand to accommodate the deformation. The modulation scheme and expanded bandwidth reduce the potential impedance mismatch between the receiver and transmitter. This antenna can accommodate 28% and 30% strain in the horizontal and vertical directions, respectively. The coupling efficiency and output power decrease by 7% and 2% for 28% strain in the horizontal direction and by 12% and 3.6% for 30% strain in the vertical direction, respectively. Similarly, multichannel antennas with multiple serpentine lines allow independent

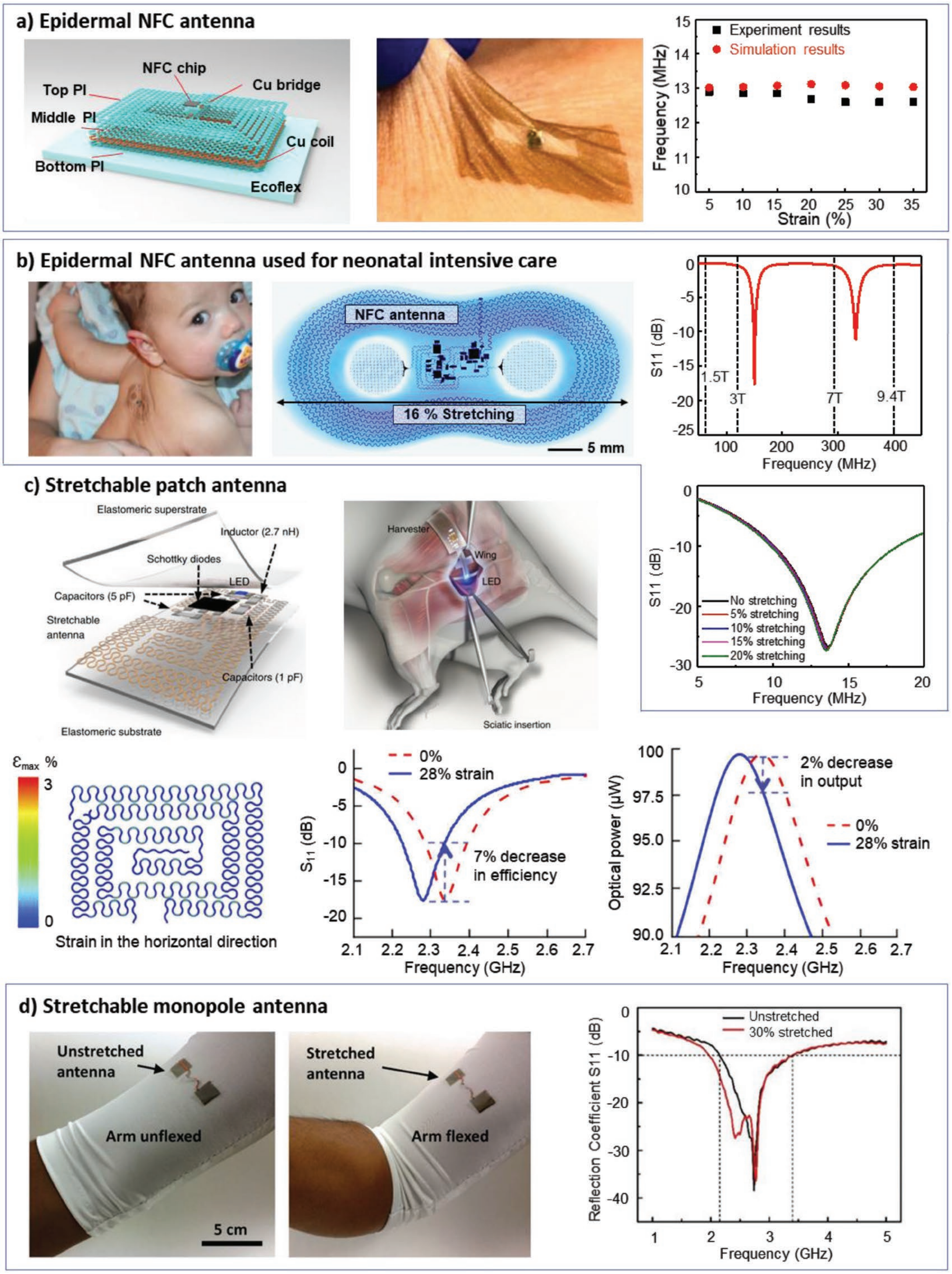

Figure 1. Stretchable antennas based on serpentine structures. a) Schematic illustration of each layer of a skin-mounted, epidermal NFC antenna. Under extreme deformations, the measured and simulated frequencies exhibit only small changes. Reproduced with permission.[40] Copyright 2014, Wiley-VCH. b) A related epidermal NFC antenna used in neonatal monitoring, compatible with mounting in areas where the skin undergoes large deformations due to wrinkling (back of the infant). The gain of the antenna remains relatively the same after it undergoes ≈20% stretching. The resonant frequency is designed to be different from those of MRI scanners commonly used in hospitals to avoid any interference. Reproduced with permission.[76] Copyright 2019, AAAS. c) A stretchable patch antenna used as a power harvester in an implantable optoelectronic device designed for optogenetic studies in small animal models. The antenna performance (S_{11} and optical power output) changes only slightly (less than 8%) due to a horizontal strain of 28%. Reproduced with permission.[77] Copyright 2015, Springer Nature. d) A stretchable monopole helical antenna can accommodate basic motions of the arm. Stretching to a strain of 30% leads to a decrease and an increase in frequency and bandwidth, respectively. Reproduced with permission.[82] Copyright 2015, Wiley-VCH.

modulation of power and operation of separate light sources, simply through adjustments in the transmitted frequency.[78,79] A three-channel antenna of this type has an overall size that is ≈60% smaller than an otherwise similar system with three separate antennas. The multichannel system consists of four serpentine lines that form three capacitively coupled channels tuned at 2.3, 2.7, and 3.2 GHz, respectively.[79] For a uniaxial strain of 30%, the center frequency of the channels shifts to 2.1, 2.4, and 2.8 GHz like the antenna with single serpentine line, respectively. To ensure sufficient separation between the frequencies of these channels, the system includes advanced impedance matching techniques that minimize cross-coupling and control the separation (0.4–0.8 GHz) to prevent adverse effects on performance.[77] In another demonstration, a wireless antenna with two independent channels at 1.8 and 2.9 GHz serves as the basis of systems for independently controlled optical stimulation and drug delivery.[78] Stretching the antenna uniaxially and biaxially by 20% creates maximum strains in the copper traces of ≈1% and only slight shifts (≈30–100 MHz) in the center resonant frequency, thereby ensuring a stable operation.

Related concepts can serve as the basis of far-field RF power harvesters that include a modularized collection of ultrathin antennas, rectifiers, and voltage doublers, with applications in epidermal devices.[80] Here, a one-loop antenna consists of circular serpentine metallic mesh structures that yield elastic mechanical properties. The gain reaches ≈2.89 dB in air for an operating frequency 1.65 GHz. Similar serpentine metallic mesh layouts can also be used in tunable far-field dipole antennas that operate at 1.7 GHz for 0% stretching and 1.56 GHz for 20% stretching.[81] Simulated distributions of surface currents at 10% stretching suggest that sufficient power can be harvested for practical applications in battery-free implanted systems.

As an initial attempt at 3D designs, Figure 1d shows a macroscopic, helical spring monopole antenna that operates at 2.45 GHz.[82] The helical geometry relieves the strains/stresses in the metal layer to afford an elastic stretchability of ≈30%. The gains of the unstretched and stretched antennas are 0.05 and 0.7 dB, respectively. After 30% stretching, the reflection coefficient of the antenna on the skin slightly shifts from –24 to –27 dB and the resonant frequency shifts from 2.45 to 2.2 GHz.

3. Antennas Based on 3D Assembly

The controlled assembly of complex 3D micro/nanostructures provides access to advanced classes of stretchable antennas, as extensions of the example in Figure 1d.[83] The process involves strain relaxation in an elastomeric substrate to trigger simultaneous in-plane and out-of-plane translational and rotational motions in a 2D precursor to form a corresponding 3D mesostructure. The transformation from 2D to 3D is governed by the 2D layout and the mechanical properties of the precursor, the locations for bonding at the precursor/substrate interface, and the magnitude of the prestrain. 3D helical structures formed in this way have considerable enhancements (approximately two times) in elastic stretchability when compared to 2D serpentine interconnects of the type described in the previous section.[84] These helices are characterized by a spring-like response and uniform stress distribution, while the serpentines are dominated by buckling or scissor-like mechanics.[85] 3D helical structures bonded to an elastomeric substrate (E = 20 kPa) and encapsulated with an ultralow modulus elastomer (E = 3 kPa) can provide highly stretchable mechanics.[84] A typical system offers ≈140% uniaxial and ≈70% biaxial elastic stretchability where the maximum computed stress in the metal layer is ≈130 MPa, well below the yield stress (357 MPa) for copper. Additionally, a two-stage encapsulation technique can further increase the stretchability, as in the design of the NFC antenna shown in **Figure 2**a.[86] Here, the encapsulation occurs while the system is still partially prestrained, in a way that enhances the stretchability by a factor of 4 compared to that obtained by the standard approach with an elastomeric substrate (E = 20 kPa) and an ultralow modulus encapsulating elastomer (E = 3 kPa). The NFC antenna with 3D helical structure can be stretched uniaxially by 102% and biaxially by 94% before reaching the yield point of the copper. The simulated and measured values of S_{11} remain stable for ≈50% uniaxial stretch.[86] NFC antennas with 3D structures offer enhanced Q factor and improved working angles compared to standard 2D designs,[87] as in the example of the 3D spiral NFC antenna in Figure 2b.[88] This system can be designed with a broad range of frequencies and it can produce twice the induced voltage compared to an otherwise similar 2D coil across a working angle α between 0° and 50°. The antenna can be reversibly tuned by controlling strains applied to the elastomeric substrate.

Figure 2c shows an additional example of an NFC antenna based on the 3D assembly.[89] Cuts, slits, and openings in 2D precursors help to determine, along with the predetermined bonding sites, the final geometrical shape of the resulting 3D structure and its RF properties. This antenna has an operating frequency that shifts to a higher resonant frequency (from 12.29 to 14.6 MHz) as the initial, 100% prestrain in the supporting elastomer releases to induce the 2D–3D geometric transformation. The reversible tuning capabilities are useful in accounting changes in electromagnetic properties of the surroundings, of particular importance in devices that mount on or lie close to the skin. The highly customizable 3D shapes create a set of opportunities in properties, size, and tunability.

Size, in particular, is important in wearable and/or biointegrated systems. Electrically small antennas (ESA) are defined by an electrical sizes that are less 0.5,[90] where the size corresponds to the product of the free-space wave number of the RF waves at the operating frequency and the radius of the smallest sphere that circumscribes the antenna. ESAs are of particular interest due to their large bandwidths and increased data transmission rates. However, typical ESAs operate at a fixed frequency and cannot deform. Volumetric ESAs show a higher efficiency/bandwidth than that of planar ESAs due to their large volume occupation. Mechanically guided 3D assembly can be used to create ESAs with significantly reduced sizes.[90] The meander-line-based hemispherical ESA (MHESA) and helix-based hemispherical ESA (HHESA) shown in Figure 2d maintain a stable frequency after a cyclic force, as an illustration of the combined deformability and robustness of operation. Volumetric ESAs can be tuned for different working frequencies, in a manner analogous to the examples described previously. The MHESA shown here operates at 1.08 GHz, and shifts to 0.94 GHz for

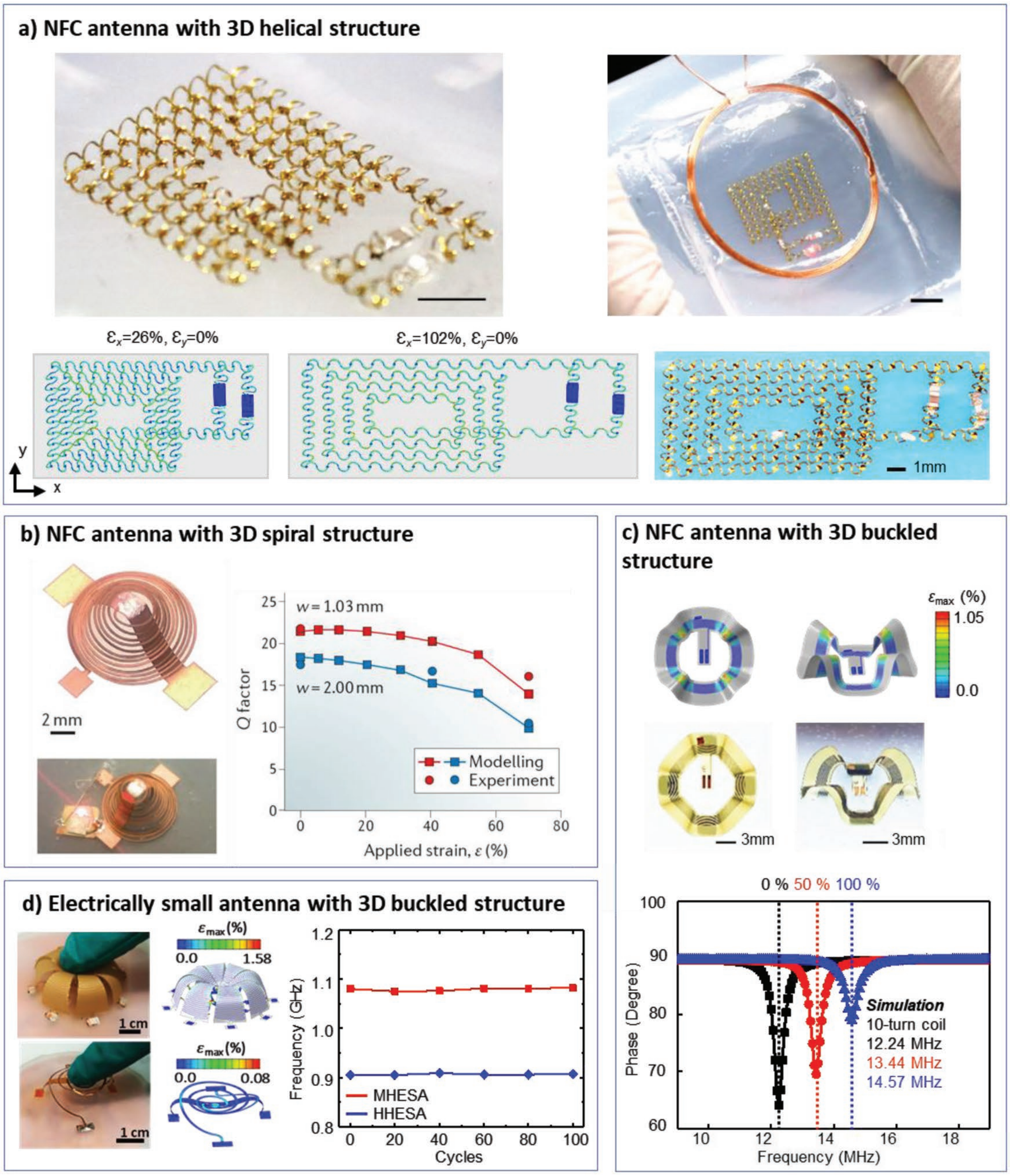

Figure 2. Stretchable antennas formed by 3D assembly. a) Perspective view of a 3D soft antenna consisting of helical mesostructures with one-stage and two-stage solid encapsulation processes. The device can function under uniaxial/biaxial stretching. Finite element analysis (FEA) of structures with one-stage and two-stage encapsulation reveals the Mises stress distributions after ≈102% uniaxial strain. Reproduced with permission.[86] Copyright 2019, Wiley-VCH. b) The Q factor of a 3D NFC spiral antenna increases with decreasing trace width and decreases by ≈35% under a strain of 70%. Reproduced with permission.[88] Copyright 2016, AAAS. c) The 3D NFC buckled antenna system undergoes a shift in resonant frequency after the prestretched silicon elastomer is gradually released. Reproduced with permission.[89] Copyright 2018, Wiley-VCH. d) The meanderline-based hemispherical ESA (MHESA) and helix-based hemispherical ESA (HHESA) maintain a constant resonant frequency after 100 cycles of pressing and unloading. FEA simulations reveal the magnitude of maximum principal strain in the copper layer after deformation. Reproduced with permission.[90] Copyright 2019, Wiley-VCH.

30% applied strain. The HHESA operates at 0.9 GHz, and shifts to 0.82 GHz for 38% applied strain. These and other demonstrations indicate that mechanically guided 3D assembly represents a broadly promising technique that can be used to create functional, tunable, and highly stretchable antennas for a range of applications.

4. Antennas Based on Textiles

Textile antennas represent an interesting alternative configuration that replaces the stretchable elastomer with fabrics, of particular utility in clothing around the areas of the arms and legs where high levels of deformations can occur. The electromagnetic performance of these types of antennas is primarily influenced by the material properties and weaving patterns of the conductive fibers.[42,91] Designs must consider that the mechanical and electrical properties of the fabrics often change during deformation.[44,91] Accurate engineering simulations can be challenging because assumptions that the material properties remain constant can produce misleading results. For example, variabilities in the positions of the threads, the air gaps between fabrics, and the distance to the body introduce additional uncertainties. Approaches that use effective material properties, defined empirically by experiment, must typically be used.

For textile antennas, there are configurations that replace the dielectric substrate with a textile substrate but keep metallic components, and an alternative design is to replace both the dielectric substrate by a textile substrate and the metallic components by conductive fabrics to achieve an all-textile design.[44,47,92,93] In one report, orthogonal weaving technology yields 3D microstrip fabric antennas (3DFA) as shown in **Figure 3**a.[94] The 3DFA can be flexed at different radii of curvature parallel and perpendicular to the feeding direction, as shown in Figure 3b. The resonant frequency remains stable at ≈1.5 GHz for both the parallel and perpendicular feeding directions. Figure 3c,d indicates that the return loss slightly decreases for parallel and perpendicular feeding directions, but it remains in an acceptable range below −10 dB.

Four purely textile patch antennas with resonant frequencies of 2.4 GHz can support Bluetooth wearable applications with good performance during mechanical deformation.[44] The antenna geometries involve truncated corners to enhance operation with circular or linear polarization, and spacer substrates with 3.5 and 6 mm heights, respectively. The four antennas include a linear polarized antenna on a felt substrate (LF), circular polarized antenna on a felt substrate (CF), linear polarized antenna on a spacer substrate (LS), and a circular polarized antenna on a spacer substrate (CS). The LS and CF antennas exhibit the best return loss at −30 and −24 dB, respectively. Experimental measurements define the change in resonance frequencies for the LS and CF antennas as a function of the radius of curvature for bending parallel and perpendicular to the feeding direction. As the radius decreases from 100 to 35 mm, the normalized change ($f_{\mathrm{radius}}/f_{\mathrm{flat}}$) in resonant frequency for the LS and CF with a parallel feeding direction is small (0.98–1.01). For the LS and CF with a perpendicular feeding direction, the normalized frequency decreases to 0.93 as the radius of curvature approaches 35 mm. Two such textile antennas can be used in a magnetic resonance–coupled system for wireless high-power transmission.[95] A conductive threat embroidered in cotton forms a textile receiver antenna and a flexible polymer substrate features the stranded metallic wire transmitter antenna. These antennas maintain an output power close to 12 mW at a working distance of 15 cm. Conductive silver filaments in the threads of the receiver antenna enhance its electrical properties. After bending, the S_{11} parameter slightly decreases (≈10%) for a 50 mm bending radius and maintains a stable resonant frequency at 6.78 MHz. Robust designs in ballistic textile patch antennas and careful material selections for them provide sufficient endurance for L-band satellite communications operating at 1616–1626.5 MHz in

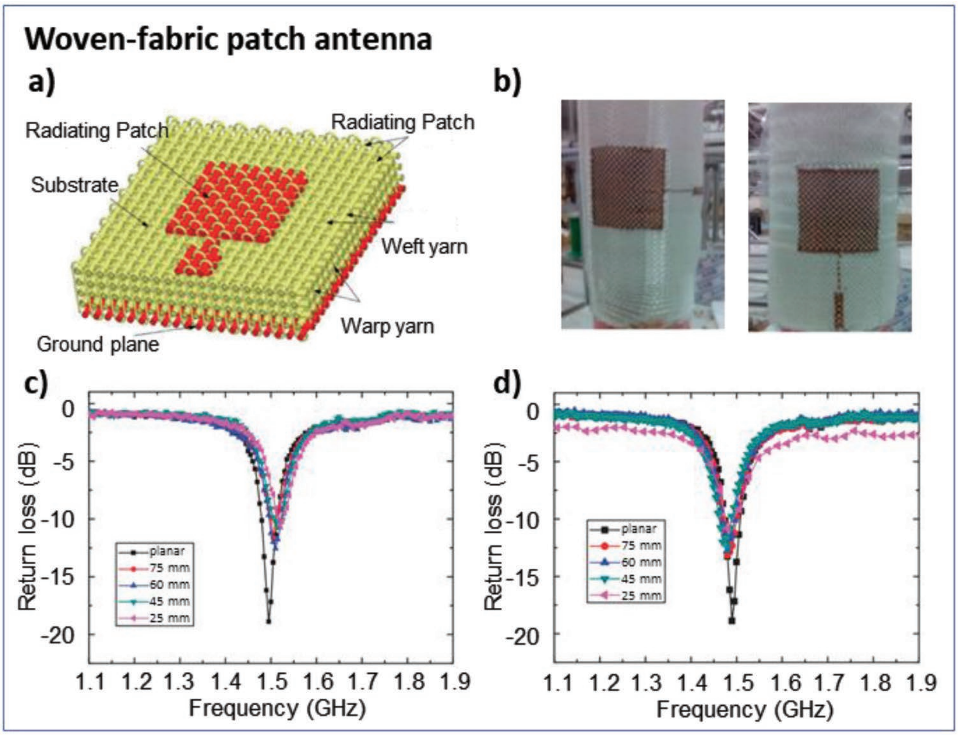

Figure 3. Stretchable antennas in woven fabric. a) 3D woven fabric microstrip patch antenna (3DFA). b) The feeding line of a 3DFA cylindrical patch antennas can be placed parallel or perpendicular to the curvature direction. The return loss (dB) of the 3DFA decreases with radius of curvature in these two configurations. c) Parallel to the feeding direction and d) perpendicular to the feeding direction. The performance remains relatively stable for radii of curvature between 25 and 75 mm. a–d) Reproduced with permission.[94] Copyright 2017, SAGE.

harsh/extreme temperature (−10 °C) and humidity environments.[96,97] The center resonant frequencies of dry, frozen (−10 °C), and soaking wet antennas of this type are 1.6, 1.23, and 0.88 GHz respectively. After drying the wet and the frozen antennas, the center resonant frequency shifts back to 1.6 GHz for reliable operation with global positioning systems. The comfort and ease of integration with clothing are attractive features of textile antennas for wearable applications. Precise control of the embroidering resolution and manufacturing process is, however, required to realize levels of performance comparable to those of conventional copper counterparts.[43] Further improvements in strategies for the manufacture/embroider of conductive fibers into high-performance textile antennas may facilitate the broader use of such antennas in practical applications of wearable electronics systems.

5. Antennas Based on Liquid Metal

The attractive mechanical, electromagnetic, and chemical properties of gallium-based liquid metals make them safe-to-handle, reliable candidates for flexible and stretchable electronic devices and radio-frequency communication platforms.[48,98,99] Liquid metal patterning in thin films and in soft microfluidic networks allows for the construction and characterization of many types of antennas. Published demonstrations include NFC antennas,[100,101] monopole,[102,103] dipole,[50,104–109] patch,[28,110–112] and planar inverted cone, miniaturized inverted *F*, and unbalanced loop radiofrequency antennas,[113–115] among others. The advantages of these types of devices are that the encapsulating elastomer determines the mechanical performance, while the liquid metal can support nearly unlimited levels of strain without any significant resistance to deformation due to the ability to flow in a liquid state.[48]

Figure 4a shows a patterned GaInSn (Gallistan) NFC antenna that can be stretched up to ≈30% with a stable Q factor and resonant frequency of ≈13.56 MHz. A system constructed with this type of antenna can be mounted on the wrist, throat, and joints between the fingers where a change in output voltage accurately captures the motion/deformation. Similar antennas can be constructed from gallium–indium eutectics (EGaIn) for flexible telemetry with electromagnetic performance that can support transfer of both data and power.[101] The Q factor of a recently reported NFC antenna with EGaIn is ≈30% less that the otherwise similar antenna built in the conventional way since the conductivity of the liquid metal is about one order of magnitude lower than that of copper/gold. At an operating frequency of 4 MHz, this difference corresponds to an ≈46% reduction in power transfer efficiency.

Generally, the resonant frequency of a stretchable dipole/monopole antenna will shift as a result of mechanical deformation. This behavior can be viewed as a tuning mechanism, as described previously, or it can be exploited as a strain sensor.[116] The reversibly deformable dipole antenna shown in Figure 4b can be mechanically tuned from a resonant frequency of 1600–1900 MHz by applying ≈20% uniaxial strain.[50] The antenna radiates with a high efficiency (≈90%) and can serve as a means for wireless strain monitoring where the antenna additionally serves as the sensor. Specifically, a monopole antenna connected to a pumping apparatus allows for dynamic adjustments of the length of the antenna, thereby shifting the resonant frequency between 1.7 and 4.9 GHz.[103] Electrochemically controlled capillarity (ECC) can also be used to shift the resonant frequency and reflection coefficient of a monopole antenna between 0.66 GHz (−37 dB) and 3.4 GHz (−8 dB) by providing a small DC voltage to control the flow direction and volume of the liquid metal inside the microchannel.[102] Alternatively, a pressure approach can shift the frequency of a liquid metal dipole antenna in a manner that exploits the thin oxide skin of EGaIn to restrict the liquid flow and limit the initial electrical length of the antenna into a predefined geometry.[104,117] When an applied pressure exceeds the yield stress (≈7 psi) of the thin oxide skin, the liquid metal begins to flow, thereby increasing the length of the antenna an shifting the frequency from 3.2 to 2 GHz as the microchannel fills.

Tunability can be an advantage in many instances, but stability in operation during deformations is an important feature for most biointegrated applications. To achieve highly stable operation in dipole antennas built with liquid metal, the geometrical parameters (aspect ratio) of the straight/serpentine channels must adjust to changes in length due to mechanical deformation.[106] Specifically, the aspect ratio (α) of a serpentine half-wave dipole antenna with liquid metal can be optimized to maintain a stable resonant frequency under stretching, bending, and twisting as shown in Figure 4c (middle). Figure 4c (right and left) highlights the potential wearable locations of the antenna and compares the frequency stability between a serpentine and straight antenna under a dynamic applied strain of ≈50%. For serpentine geometries with $\alpha > 1$, 40% uniaxial strain causes an increase in the return loss from −15 to −48 dB.

Figure 4d shows a liquid metal planar inverted cone antenna (PICA) that retains its functionality during high levels of multiaxial stretching.[113] This PICA is foldable and conformal and has an ultrawideband (UWB) frequency range (3.1–10.6 GHz). Even for 40% stretching along the horizontal or vertical axis, the reflection coefficient maintains at least −10 dB. Additionally, the device exhibits a monopole radiation pattern in the low-frequency range and an omnidirectional radiation pattern in the high-frequency range. Improving the performance of liquid metal antennas to levels that compare favorably to those of similar solid metal antennas will require further work to address the surface oxides and to improve the conductivity.

6. Antennas Based on Nanomaterials

Many active research efforts focus on the integration of conductive nanomaterials such as metal NWs and CNTs into flexible and stretchable electronic systems. Nanomaterials can support flexibility, tunability, durability, and performance across a wide range of antenna configurations, with demonstrations that include patch,[118] NFC,[119] dipole,[120–122] and monopole designs.[53] As an example, the stretchable mechanics of "wavy" networks of Ag-NWs allows for interesting classes of tunable and transparent RF antennas.[123] The procedure shown in **Figure 5**a highlights a ≈30% uniaxial precompression step to create networks of this type with different areal densities, for subsequent transfer onto a polymer substrate.[124]

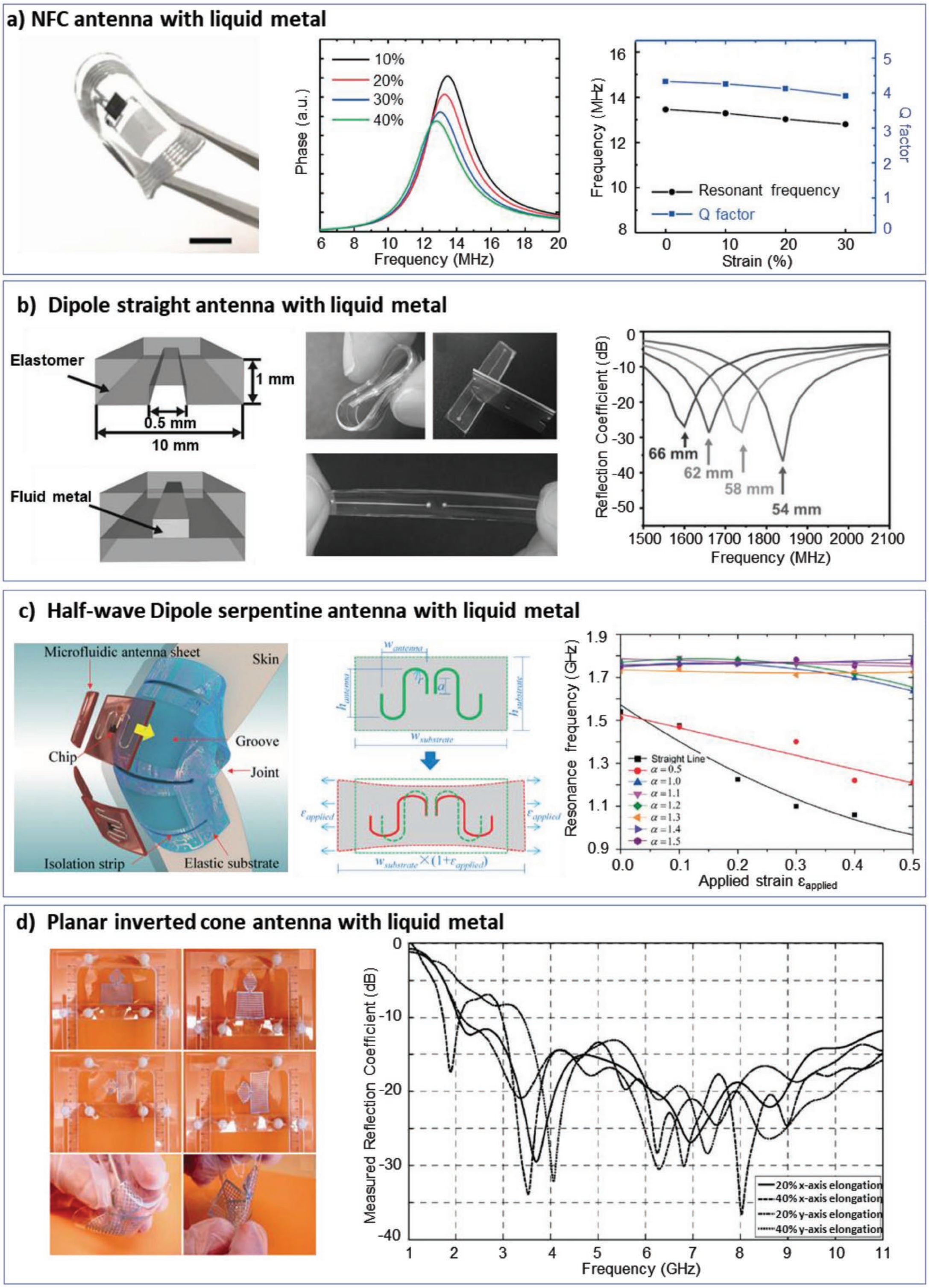

Figure 4. Stretchable antennas based on liquid metals. a) An NFC coil antenna formed with patterned liquid metal experiences a slight decrease in phase, resonant frequency, and Q factor after ≈30% strain. Reproduced with permission.[100] Copyright 2017, Springer Nature. b) A reversibly deformable dipole liquid metal antenna can be tuned to a desired resonant frequency by stretching the elastomer. The reflection coefficient (dB) remains relatively constant for applied strains between ≈7% and ≈20%. Reproduced with permission.[50] Copyright 2009, Wiley-VCH. c) A half-wave dipole antenna can operate on parts of the human body which undergo large deformations such as joints. The serpentine designs provide a stable resonant frequency for applied strains of ≈50%, unlike designs that involve straight-line configurations. Reproduced with permission.[106] Copyright 2014, Royal Society of Chemistry. d) A planar inverted cone antenna can be folded and stretched by ≈40% in horizontal and vertical directions while maintaining good impedance match defined by $S_{11} = -10$ dB within the 3–11 GHz frequency range. Reproduced with permission.[113] Copyright 2009, IEEE.

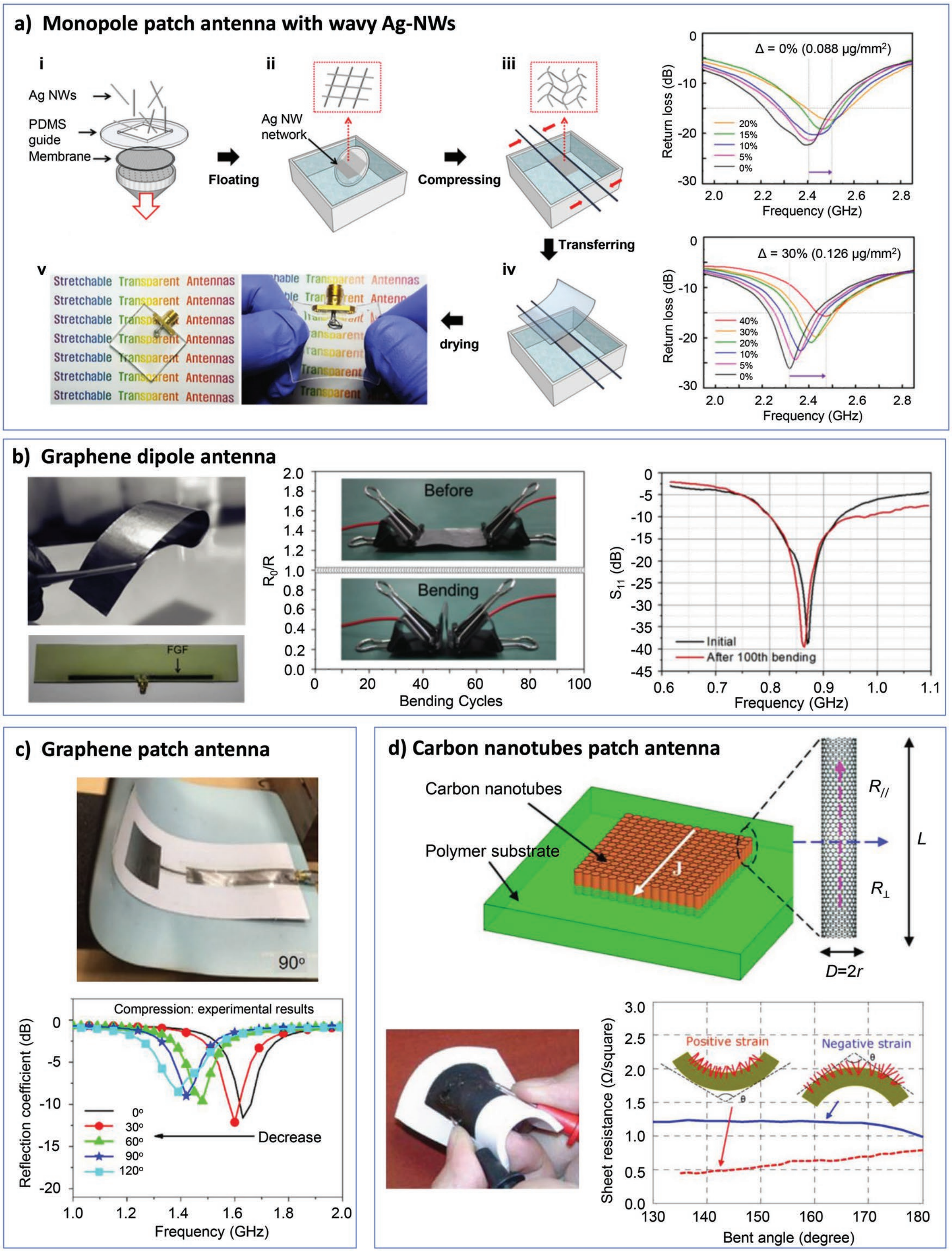

Figure 5. Flexible and stretchable antennas based on nanomaterials. a) The use of wavy AgNWs allows for enhanced performance and tunability in patch antennas due partly to the high areal density of AgNWs and ability to be stretched up to ≈40%, with return loss (dB) that is superior to analogous devices built with nonwavy AgNWs. Reproduced with permission.[124] Copyright 2016, American Chemical Society. b) A flexible graphene film (FGF) yields a dipole antenna with performance comparable to that of a rigid copper antenna, and with a weight that is five times lower. The FGF antenna retains its original resistance and return loss (S_{11}) after 100 bending cycles. Reproduced with permission.[126] Copyright 2018, Elsevier. c) The strain sensitivity of a graphene patch antenna outperforms that of a similar copper device after compressive and tensile bending. The frequency of the antenna decreases as the compressive bending angle increases up to 120° and the reflection coefficient decreases after 60°. Reproduced with permission.[127] Copyright 2018, Elsevier. d) A vertically aligned carbon nanotube patch antenna sheet transferred onto a polymer substrate offers high flexibility. The DC resistance varies between positive and negative strains during bending. Reproduced with permission.[130] Copyright 2010, IEEE.

Such antennas can support ≈40% uniaxial strains, 20% more than otherwise similar antennas that use planar (non-wavy) AgNWs, and 300 stretching cycles, 400% more than the planar case, while maintaining a return loss of at least −15 dB. The tunability of the antenna depends on the stretchability and the areal density of the AgNW networks. A wavy configuration provides a slightly greater range (2.31–2.47 GHz) than the planar (2.21–2.31 GHz).

Lingnan et al. developed a far-field monopole patch antenna and a 2-element patch array antenna with AgNWs to enhance the stretchability and tunability for operation at 3 and 6 GHz, respectively.[125] The dimensions of the 2-element array configuration increase the directivity from 4.16 to 8.14 dB and bandwidth from 88 to 330 MHz when compared to the monopole patch. For 15% uniaxial strain, the resonant frequency of the monopole shifts from 2.95 to 3.08 GHz and the return loss (dB) falls below the −15 dB threshold for reliable operation. The scalability and dimensions of patch antennas remain as significant challenges in integration into small stretchable systems.

Carbon nanomaterials are also attractive choices. In one example, a thermal treatment approach enhances the mechanical properties of flexible graphite film (FGF) dipole antennas shown in Figure 5b and coplanar antennas for UWB applications.[126] The dipole FGF can undergo cyclic bending without significant degradation after 100 bending cycles and shows an S_{11} of −30 dB, which compares well to an equivalent rigid copper antenna with an S_{11} of −40 dB. Additionally, the FGF coplanar antenna maintains an acceptable −10 dB bandwidth across the 3.1–10.6 GHz frequency range with minimum change in performance after bending in vertical and horizontal directions.[126] Figure 5c shows an FGF patch antenna gradually bent by 120° and the degradation in performance that begins at 60°.[127] The deformability enables approximate conformal contact with skin and relatively stable operation. Highly flexible multilayer carbon-based antennas can also be used in NFC systems. Graphene-based paper can replace metallic components of antennas to offer high levels of flexibility, stable operation upon bending fatigue.[128]

Hybrid nanomaterial systems are also of interest. In one example, such approaches yield three loop antennas (reader, receiver, and sensing) for monitoring gas concentrations while laminated in the surface of a leaf.[129] These hybrid AgNW–graphene antennas combine the properties of nanomaterials to yield a highly stretchable, transparent wearable sensor (antenna) with a stable performance during stretching up to strains of 20%.

Another nanomaterials' strategy involves the use of vertically aligned CNTs in patch antennas via transfer onto polymer substrates. The CNTs can undergo 13% stretching and bending to an angle of 130° while maintaining a good performance, as shown in Figure 5d. The DC resistance of the carbon sheet remains relatively unchanged for negative strain and it increases proportional to bending angle for positive strain.[130] Also, the gain (dB) of the conformal CNT patches remains constant in the *H*-plane at (2.25 GHz) and decreases for the *E*-plane (1.95 GHz). Comparisons of the performance of three 2.45 GHz wearable monopole antennas made of graphene, CNTs, and copper suggest that the graphene and CNT configurations maintain acceptable return loss with a small (≈10%) reduction compared to the copper antenna.[131] A voxel human model can be used to simulate the degradation in performance, the half-sphere radiation pattern, and the specific absorption rate (SAR) when mounted onto the body. Such simulations are very valuable as design tools to guide optimization of stretchability without compromising performance.

7. Conclusion and Future Perspectives

7.1. Conclusion

Roadmaps constructed around miniaturization of electronics continue to dominate research and development in this area of technology. Biointegrated devices represent a parallel path where miniaturization continues to be important, but where fundamentally new capabilities arise as a result of a shift from rigid and planar physical forms to soft, conformal biocompatible embodiments. This transition demands innovative ideas in material science with creative engineering solutions in mechanical and electromagnetic designs. The antenna is a critical component of many of the most important envisioned applications. The strategies highlighted in this review include the use of unusual materials such as liquid metals, nanowires, and woven textiles and of optimally configured 2D/3D structures of conventional materials. The choice of approach often depends on the application. The performance of flexible and stretchable antennas is summarized in **Table 1**. The operating frequency, bandwidth, and the effect of mechanical deformations are compared for various different fabrication methods/materials. Configurations that exploit geometric structures focus on enhancing the stretchability and improving the electrical performance, with a broad range of examples of operation in the HF and UHF ranges for personal area networks. Extensive experimental and computational studies reveal various considerations in choices of shapes and layouts as design guidelines to meet requirements in mechanical and electromagnetic characteristics. 3D assembled structures represent qualitative extensions of corresponding 2D configurations. The textile embroidered antennas described in this review focus primarily on the patch configuration. These systems have natural synergies with other work in the integration of electronics into clothing. Liquid metal traces encapsulated in soft microfluidic networks combine the excellent electrical and versatile mechanical properties of gallium alloys to yield monopole, dipole, patch, and NFC antennas. Techniques for patterning liquid metals offer a breadth of choices in straight or serpentine designs that provide tunable or stable operation, respectively. Nanomaterials such as NWs, graphene, and carbon nanotubes, mounted on or embedded in elastomeric polymers, can be used to construct stretchable antennas with electrical performance that can compare with that of conventional devices. Examples include devices that use the substrate to increase the dielectric properties and that exploit designs for high-speed communications and low-power operation. These nanomaterials as well as combinations of them support an extensive set of options for specific antenna types. In all cases, the rich scope of topics in materials science, mechanical engineering, electrical

Table 1. Summary of the performance of representative stretchable and flexible antennas.

Antenna types	Strategies	Operating frequencies	Bandwidth (S_{11} < −10 dB)	Performance under stretching/bending	Applications
Epidermal NFC antenna[76]	Metal–serpentine structures	≈13.56 MHz	≈7.5 MHz	Negligible $\Delta f^{a)}$ and $\varepsilon^{b)}$<0.3% for 16% stretching/negligible Δf and ε <0.3% for $R^{c)}$> 140 mm	Communication and energy harvesting
Patch antenna[77]	Metal–serpentine structures	≈2.34 GHz	≈200 MHz	Δf increases <100 MHz and ε < 3% for 28% stretching	Energy harvesting
Monopole helical antenna[82]	Metal–serpentine structures	≈2.45 GHz	≈1.2 GHz	Δf decreases <230 MHz for 30% stretching	Communication
NFC antenna with 3D spiral structure[88]	3D assembly	≈13.56 MHz	–	Achieves ≈70% stretching	Energy harvesting
NFC antenna with 3D buckled structure[89]	3D assembly	≈12.24 MHz	–	Δf decreases <2.33 MHz for 100% stretching	Communication and energy harvesting
3D electrically small antenna MHESA[90]	3D assembly	≈1.08 GHz	≈135 MHz	Δf decreases <145 MHz and ε < 1.58% for 30% stretching	Communication
Woven-fabric patch antenna[94]	Textiles (3D orthogonal woven fabric)	≈1.52 GHz	≈300 MHz	Δf decreases <40 MHz for R > 25 mm	Communication
NFC antenna[100]	Liquid metal (GaInSn)	≈13.56 MHz		Δf decreases <0.76 MHz for 30% stretching	Strain sensor and communication
Dipole straight antenna[50]	Liquid metal (EGaIn)	≈1.85 GHz	≈250 MHz	Δf decreases <0.25 GHz for 40% stretching	Strain sensor
Half-wave dipole serpentine antenna[106]	Liquid metal (EGaIn)	≈1.75 GHz	≈90 MHz	Negligible Δf for 50% stretching with the aspect ratio $\alpha = 1.5$ (Figure 4c)	Communication
Planar inverted cone antenna[113]	Liquid metal (Galinstan)	≈3–10.6 GHz	Ultrawideband	Relatively stable within ≈40% stretching (Figure 4d)	Communication
Monopole patch antenna[124]	Nanomaterials (wavy AgNWs)	≈2.34 GHz	≈290 MHz	Δf decreases <160 MHz for 40% stretching	Communication
Graphene dipole antenna[126]	Nanomaterials (graphite)	≈865 MHz	≈160 MHz	–	Communication
Graphene patch antenna[127]	Nanomaterials (graphite)	≈1.63 GHz	≈200 MHz	Δf decreases <157 MHz for R > 55 mm	Strain sensor
Carbon nanotube patch antenna[130]	Nanomaterials (CNTs)	≈2.25 GHz	≈150 MHz	Δf decreases <300 MHz for R > 32 mm	Communication

a)Δf: Frequency shift; b)ε: Strain in metal layer; c)R: Bending radius.

engineering, and manufacturing in the context of rapidly growing, uniquely enabled applications wearable devices, biointegrated systems, and other areas suggest promising opportunities for research that can complement activities in conventional electronics technologies.

7.2. Future Perspectives

As this frontier area of research continues to develop, so will innovative ideas in materials and designs for antennas with improved performance in wireless communication, control, and power transfer. Miniaturization directly impacts the bandwidth, gain, radiation efficiency, and working frequencies. Geometrical approaches that exploit helical, spiral, fractals, and serpentine structures introduce large radiating structures into a fixed spaced or volume, where a compact design is preferred.[132] Manipulating the substrate thickness also serves as a means to tune the antenna performance. Thin elastomeric substrates are advantageous in terms of flexibility and deformability but they offer limited isolation from the dielectric properties of the surroundings which, for air, leads to requirements in large antenna sizes. Thick substrates impose mechanical constraints to mechanical deformation but they provide isolation and facilitate size miniaturization. Adding perforations to the substrate can mitigate the mechanics disadvantages of thick substrates with high dielectric constants,[133] but the locations of these perforations can affect the operating frequency. The emergence of 5G technologies and its application in the millimeter wave band (>28 GHz) offers significantly enhanced communication speeds with transformational potential in consumer, industrial, and military systems, where many opportunities for flexible/stretchable antenna designs exist.[134] However, the millimeter wave band frequency will feature highly directional antennas with concentrated RF energy that requires extensive investigation to control exposure to high power density and consequently high SAR for the human body.[134] In these and other cases, biointegrated implantable systems that operate completely/partially inside electromagnetically lossy biofluids and tissues require additional considerations associated with the physiological loads and the influence of the surroundings. Small antenna sizes, biocompatible encapsulation layers, sufficient bandwidths for data transmission, and high radiation efficiencies are essential considerations. Biocompatible insulation layers can be inserted between the antenna and surrounding biofluids/tissues to mitigate losses in the near-field range.[135] Careful engineering designs for these layers and the associated antennas can reduce the mismatch between the biological system and surrounding free space for increased power transmission within constraints associated with regulations on SAR.[135]

Engineered 2D/3D structures allow for simple as well as highly complex and tunable systems, although enhanced structural complexity does not necessarily lead to improved performance. Additional research will establish means for selecting optimal structures for desired operating frequencies and performance attributes, where the effects of the adjacent environment and the circuit itself are considered explicitly. For textile antennas capable of large deformations, enhancements in the techniques for embroidery, improvements in the materials for conductive threads, and reductions in the overall sizes are of interest. Scalability in manufacturing and capabilities in miniaturization demand additional advances in the processes and materials. Further research may define specialty fabric coatings to mitigate effects of water and moisture, to enable washing and to support proper function in extreme environments, without changes in frequency or bandwidth.[136,137] A main challenge for antennas constructed with the most common liquid metals for this purpose follows from detrimental effects of the thin oxide layer that forms spontaneously when exposed to oxygen in the air. Schemes to eliminate leakage of these liquids from their containment structures and to enable manipulation of the liquid metal inside the structures represent additional areas for further study. Advances in nanomaterials approaches may be relevant for tailored coatings and laminates that can be deployed with other antenna fabrication/material strategies. Stretchable structures and nanomaterial-enabled stretchable conductors that use doped NWs and CNTs for high electrical conductivity and optical transparency can be used in flexible antennas with enhanced electromagnetic performance. 3D microscale coils inspired by biological templates can serve as stretchable conductors with large deformability and stable conductivity.[138] Such coils can direct deformations in the supporting substrate out of plane to allow for large levels of strechability with only small strains the materials of the coils and high radiation efficiencies (>95%). Additional work in nanoscale design will expand opportunities for geometries and materials in stretchable devices with improved electromagnetic performance.[138,139] In these and other cases, theoretical and computational models will accelerate and guide the development process, particularly for systems that feature unconventional materials or a combination of strategies in nanomaterials and conventional conductors.

Acknowledgements

Z.X. and R.A. contributed equally to this work. This work was supported by the National Natural Science Foundation of China (Grant No.11402134), National Science Foundation Graduate Research Fellowship (NSF grant number 1842165), Ford Foundation Predoctoral Fellowship, and NSF (CMMI1635443).

Note: References [7], [10], [13], [14], [39], [65], [78], [80], [81], [86], [89], [90], and [102] were corrected with the correct article numbers on April 4, 2020, after initial publication online.

Conflict of Interest

The authors declare no conflict of interest.

Keywords

antennas, flexible electronics, liquid metal, stretchable electronics, wireless communication

Received: April 30, 2019
Revised: June 16, 2019
Published online: September 6, 2019

[1] T. R. Ray, J. Choi, A. J. Bandodkar, S. Krishnan, P. Gutruf, L. Tian, R. Ghaffari, J. A. Rogers, *Chem. Rev.* **2019**, *119*, 5461.
[2] J. Choi, A. J. Bandodkar, J. T. Reeder, T. R. Ray, A. Turnquist, S. B. Kim, N. Nyberg, A. Hourlier-Fargette, J. B. Model, A. J. Aranyosi, S. Xu, R. Ghaffari, J. A. Rogers, *ACS Sens.* **2019**, *4*, 379.
[3] J. T. Reeder, J. Choi, Y. Xue, P. Gutruf, J. Hanson, M. Liu, T. Ray, A. J. Bandodkar, R. Avila, W. Xia, S. Krishnan, S. Xu, K. Barnes, M. Pahnke, R. Ghaffari, Y. Huang, J. A. Rogers, *Sci. Adv.* **2019**, *5*, eaau6356.
[4] A. J. Bandodkar, P. Gutruf, J. Choi, K. Lee, Y. Sekine, J. T. Reeder, W. J. Jeang, A. J. Aranyosi, S. P. Lee, J. B. Model, R. Ghaffari, C.-J. Su, J. P. Leshock, T. Ray, A. Verrillo, K. Thomas, V. Krishnamurthi, S. Han, J. Kim, S. Krishnan, T. Hang, J. A. Rogers, *Sci. Adv.* **2019**, *5*, eaav3294.
[5] A. Koh, D. Kang, Y. Xue, S. Lee, R. M. Pielak, J. Kim, T. Hwang, S. Min, A. Banks, P. Bastien, M. C. Manco, L. Wang, K. R. Ammann, K. I. Jang, P. Won, S. Han, R. Ghaffari, U. Paik, M. J. Slepian, G. Balooch, Y. G. Huang, J. A. Rogers, *Sci. Transl. Med.* **2016**, *8*, 366ra165.
[6] S. B. Kim, K. Lee, M. S. Raj, B. Lee, J. T. Reeder, J. Koo, A. Hourlier-Fargette, A. J. Bandodkar, S. M. Won, Y. Sekine, J. Choi, Y. Zhang, J. Yoon, B. H. Kim, Y. Yun, S. Lee, J. Shin, J. Kim, R. Ghaffari, J. A. Rogers, *Small* **2018**, *14*, 1802876.
[7] S. P. Lee, G. Ha, D. E. Wright, Y. J. Ma, E. Sen-Gupta, N. R. Haubrich, P. C. Branche, W. H. Li, G. L. Huppert, M. Johnson, H. B. Mutlu, K. Li, N. Sheth, J. A. Wright, Y. G. Huang, M. Mansour, J. A. Rogers, R. Ghaffari, *npj Digital Med.* **2018**, *1*, 2.
[8] Y. Liu, J. J. S. Norton, R. Qazi, Z. Zou, K. R. Ammann, H. Liu, L. Yan, P. L. Tran, K.-I. Jang, J. W. Lee, D. Zhang, K. A. Kilian, S. H. Jung, T. Bretl, J. Xiao, M. J. Slepian, Y. Huang, J.-W. Jeong, J. A. Rogers, *Sci. Adv.* **2016**, *2*, e1601185.
[9] S. Han, J. Kim, S. M. Won, Y. J. Ma, D. Kang, Z. Q. Xie, K. T. Lee, H. U. Chung, A. Banks, S. Min, S. Y. Heo, C. R. Davies, J. W. Lee, C. H. Lee, B. H. Kim, K. Li, Y. D. Zhou, C. Wei, X. Feng, Y. G. Huang, J. A. Rogers, *Sci. Transl. Med.* **2018**, *10*, eaan4950.
[10] S. R. Krishnan, C. J. Su, Z. Q. Xie, M. Patel, S. R. Madhvapathy, Y. S. Xu, J. Freudman, B. Ng, S. Y. Heo, H. L. Wang, T. R. Ray, J. Leshock, I. Stankiewicz, X. Feng, Y. G. Huang, P. Gutruf, J. A. Rogers, *Small* **2018**, *14*, 1803192.
[11] L. Tian, B. Zimmerman, A. Akhtar, K. J. Yu, M. Moore, J. Wu, R. J. Larsen, J. W. Lee, J. Li, Y. Liu, B. Metzger, S. Qu, X. Guo, K. E. Mathewson, J. A. Fan, J. Cornman, M. Fatina, Z. Xie, Y. Ma, J. Zhang, Y. Zhang, F. Dolcos, M. Fabiani, G. Gratton, T. Bretl, L. J. Hargrove, P. V. Braun, Y. Huang, J. A. Rogers, *Nat. Biomed. Eng.* **2019**, *3*, 194.
[12] S. Krishnan, Y. Shi, R. C. Webb, Y. Ma, P. Bastien, K. E. Crawford, A. Wang, X. Feng, M. Manco, J. Kurniawan, E. Tir, Y. Huang, G. Balooch, R. M. Pielak, J. A. Rogers, *Microsyst. Nanoeng.* **2017**, *3*, 17014.

[13] J. Kim, G. A. Salvatore, H. Araki, A. M. Chiarelli, Z. Q. Xie, A. Banks, X. Sheng, Y. H. Liu, J. W. Lee, K. I. Jang, S. Y. Heo, K. Cho, H. Y. Luo, B. Zimmerman, J. Kim, L. Q. Yan, X. Feng, S. Xu, M. Fabiani, G. Gratton, Y. G. Huang, U. Paik, J. A. Rogers, *Sci. Adv.* **2016**, *2*, e1600418.
[14] J. Kim, P. Gutruf, A. M. Chiarelli, S. Y. Heo, K. Cho, Z. Q. Xie, A. Banks, S. Han, K. I. Jang, J. W. Lee, K. T. Lee, X. Feng, Y. G. Huang, M. Fabiani, G. Gratton, U. Paik, J. A. Rogers, *Adv. Funct. Mater.* **2017**, *27*, 1604373.
[15] Y. Z. Shi, M. Manco, D. Moyal, G. Huppert, H. Araki, A. Banks, H. Joshi, R. McKenzie, A. Seewald, G. Griffin, E. Sen-Gupta, D. Wright, P. Bastien, F. Valceschini, S. Seite, J. A. Wright, R. Ghaffari, J. Rogers, G. Balooch, R. M. Pielak, *PLoS One* **2018**, *13*, e0190233.
[16] S. Y. Heo, J. Kim, P. Gutruf, A. Banks, P. Wei, R. Pielak, G. Balooch, Y. Shi, H. Araki, D. Rollo, C. Gaede, M. Patel, J. W. Kwak, A. E. Peña-Alcántara, K. T. Lee, Y. Yun, J. K. Robinson, S. Xu, J. A. Rogers, *Sci. Transl. Med.* **2018**, *10*, eaau1643.
[17] H. Araki, J. Kim, S. N. Zhang, A. Banks, K. E. Crawford, X. Sheng, P. Gutruf, Y. Z. Shi, R. M. Pielak, J. A. Rogers, *Adv. Funct. Mater.* **2017**, *27*, 1604465.
[18] S. Choi, S. I. Han, D. Jung, H. J. Hwang, C. Lim, S. Bae, O. K. Park, C. M. Tschabrunn, M. Lee, S. Y. Bae, J. W. Yu, J. H. Ryu, S.-W. Lee, K. Park, P. M. Kang, W. B. Lee, R. Nezafat, T. Hyeon, D.-H. Kim, *Nat. Nanotechnol.* **2018**, *13*, 1048.
[19] A. D. Mickle, S. M. Won, K. N. Noh, J. Yoon, K. W. Meacham, Y. G. Xue, L. A. McIlvried, B. A. Copits, V. K. Samineni, K. E. Crawford, D. H. Kim, P. Srivastava, B. H. Kim, S. Min, Y. Shiuan, Y. Yun, M. A. Payne, J. P. Zhang, H. Jang, Y. H. Li, H. H. Lai, Y. G. Huang, S. I. Park, R. W. Gereau, J. A. Rogers, *Nature* **2019**, *565*, 361.
[20] V. K. Samineni, J. Yoon, K. E. Crawford, Y. R. Jeong, K. C. McKenzie, G. Shin, Z. Xie, S. S. Sundaram, Y. Li, M. Y. Yang, J. Kim, D. Wu, Y. Xue, X. Feng, Y. Huang, A. D. Mickle, A. Banks, J. S. Ha, J. P. Golden, J. A. Rogers, R. W. t. Gereau, *Pain* **2017**, *158*, 2108.
[21] P. Gutruf, V. Krishnamurthi, A. Vazquez-Guardado, Z. Q. Xie, A. Banks, C. J. Su, Y. S. Xu, C. R. Haney, E. A. Waters, I. Kandela, S. R. Krishnan, T. Ray, J. P. Leshock, Y. G. Huang, D. Chanda, J. A. Rogers, *Nat. Electron.* **2018**, *1*, 652.
[22] G. Shin, A. M. Gomez, R. Al-Hasani, Y. R. Jeong, J. Kim, Z. Q. Xie, A. Banks, S. M. Lee, S. Y. Han, C. J. Yoo, J. L. Lee, S. H. Lee, J. Kurniawan, J. Tureb, Z. Z. Guo, J. Yoon, S. I. Park, S. Y. Bang, Y. Nam, M. C. Walicki, V. K. Samineni, A. D. Mickle, K. Lee, S. Y. Heo, J. G. McCall, T. S. Pan, L. Wang, X. Feng, T. I. Kim, J. K. Kim, Y. H. Li, Y. G. Huang, R. W. Gereau, J. S. Ha, M. R. Bruchas, J. A. Rogers, *Neuron* **2017**, *93*, 509.
[23] H. Wong, K. Luk, C. H. Chan, Q. Xue, K. K. So, H. W. Lai, *Proc. IEEE* **2012**, *100*, 2109.
[24] S. J. Chen, C. Fumeaux, B. Chivers, R. Shepherd, presented at *2016 IEEE Int. Symp. on Antennas and Propagation (APSURSI)* 26 June–1 July, **2016**.
[25] D. Cure, T. Weller, F. A. Miranda, presented at *The 8th European Conf. on Antennas and Propagation (EuCAP 2014)*, 6–11 April, **2014**.
[26] A. A. Babar, T. Bjorninen, V. A. Bhagavati, L. Sydanheimo, P. Kallio, L. Ukkonen, *IEEE Antennas Wireless Propag. Lett.* **2012**, *11*, 1319.
[27] A. A. Babar, V. A. Bhagavati, L. Ukkonen, A. Z. Elsherbeni, P. Kallio, L. Sydanheimo, *Int. J. Antennas Propag.* **2012**, *2012*, 1.
[28] G. J. Hayes, J. H. So, A. Qusba, M. D. Dickey, G. Lazzi, *IEEE Trans. Antennas Propag.* **2012**, *60*, 2151.
[29] L. H. Blumenschein, L. T. Gan, J. A. Fan, A. M. Okamura, E. W. Hawkes, *IEEE Rob. Autom. Lett.* **2018**, *3*, 949.
[30] Q. Liu, K. L. Ford, R. Langley, A. Robinson, S. Lacour, presented at *2012 6th European Conf. on Antennas and Propagation (EUCAP)*, 26–30 March, **2012**.
[31] N. Tiercelin, P. Coquet, R. Sauleau, V. Senez, H. Fujita, *J. Micromech. Microeng.* **2006**, *16*, 2389.
[32] A. Arriola, J. I. Sancho, S. Brebels, M. Gonzalez, W. D. Raedt, *IET Microwaves, Antennas Propag.* **2011**, *5*, 852.
[33] C. P. Lin, C. H. Chang, Y. T. Cheng, C. F. Jou, *IEEE Antennas Wireless Propag. Lett.* **2011**, *10*, 1108.
[34] J. Zhu, J. J. Fox, N. Yi, H. Cheng, *ACS Appl. Mater. Interfaces* **2019**, *11*, 8867.
[35] R. Bansal, *Proc. IEEE* **1984**, *72*, 989.
[36] M. Gustafsson, S. Nordebo, *Prog. Electromagn. Res.* **2006**, *62*, 1.
[37] D. H. Kim, J. H. Ahn, W. M. Choi, H. S. Kim, T. H. Kim, J. Song, Y. Y. Huang, Z. Liu, C. Lu, J. A. Rogers, *Science* **2008**, *320*, 507.
[38] D. H. Kim, J. Xiao, J. Song, Y. Huang, J. A. Rogers, *Adv. Mater.* **2010**, *22*, 2108.
[39] S. Xu, Y. H. Zhang, J. Cho, J. Lee, X. Huang, L. Jia, J. A. Fan, Y. W. Su, J. Su, H. G. Zhang, H. Y. Cheng, B. W. Lu, C. J. Yu, C. Chuang, T. I. Kim, T. Song, K. Shigeta, S. Kang, C. Dagdeviren, I. Petrov, P. V. Braun, Y. G. Huang, U. Paik, J. A. Rogers, *Nat. Commun.* **2013**, *4*, 1543.
[40] J. Kim, A. Banks, H. Y. Cheng, Z. Q. Xie, S. Xu, K. I. Jang, J. W. Lee, Z. J. Liu, P. Gutruf, X. Huang, P. H. Wei, F. Liu, K. Li, M. Dalal, R. Ghaffari, X. Feng, Y. G. Huang, S. Gupta, U. Paik, J. A. Rogers, *Small* **2015**, *11*, 906.
[41] Y. H. Jung, Y. J. Qiu, S. Lee, T. Y. Shih, Y. H. Xu, R. M. Xu, J. Lee, A. A. Schendel, W. G. Lin, J. C. Williams, N. Behdad, Z. Q. Ma, *IEEE Antennas Wireless Propag. Lett.* **2016**, *15*, 1382.
[42] Y. Ouyang, W. J. Chappell, *IEEE Trans. Antennas Propag.* **2008**, *56*, 381.
[43] A. Kiourti, J. L. Volakis, presented at *2015 IEEE Int. Symp. on Antennas and Propagation and USNC/URSI National Radio Science Meeting*, 19–24 July, **2015**.
[44] I. Locher, M. Klemm, T. Kirstein, G. Trster, *IEEE Trans. Adv. Packag.* **2006**, *29*, 777.
[45] M. Tanaka, J. Jae-Hyeuk, presented at *IEEE Antennas and Propagation Society Int. Symp. Digest. Held in conjunction with: USNC/CNC/URSI North American Radio Sci. Meeting (Cat. No.03CH37450)*, 22–27 June, **2003**.
[46] C. A. Winterhalter, J. Teverovsky, P. Wilson, J. Slade, W. Horowitz, E. Tierney, V. Sharma, *IEEE Trans. Inform. Technol. Biomed.* **2005**, *9*, 402.
[47] M. Klemm, G. Troester, *IEEE Trans. Antennas Propag.* **2006**, *54*, 3192.
[48] M. D. Dickey, *Adv. Mater.* **2017**, *29*, 1606425.
[49] I. D. Joshipura, H. R. Ayers, C. Majidi, M. D. Dickey, *J. Mater. Chem. C* **2015**, *3*, 3834.
[50] J. H. So, J. Thelen, A. Qusba, G. J. Hayes, G. Lazzi, M. D. Dickey, *Adv. Funct. Mater.* **2009**, *19*, 3632.
[51] E. Palleau, D. Morales, M. D. Dickey, O. D. Velev, *Nat. Commun.* **2013**, *4*, 2257.
[52] Y. Wu, X. Huang, L. Huang, X. Guo, R. Ren, D. Liu, D. Qu, J. Chen, *ACS Appl. Energy Mater.* **2018**, *1*, 1395.
[53] S. S. Yao, Y. Zhu, *Adv. Mater.* **2015**, *27*, 1480.
[54] Z. Chen, J. Xi, W. Huang, M. M. F. Yuen, *Sci. Rep.* **2017**, *7*, 10958.
[55] T. Kim, H. Song, J. Ha, S. Kim, D. Kim, S. Chung, J. Lee, Y. Hong, *Appl. Phys. Lett.* **2014**, *104*, 113103.
[56] J. W. Durham, Y. Zhu, *ACS Appl. Mater. Interfaces* **2013**, *5*, 256.
[57] K. S. Kim, Y. Zhao, H. Jang, S. Y. Lee, J. M. Kim, K. S. Kim, J.-H. Ahn, P. Kim, J.-Y. Choi, B. H. Hong, *Nature* **2009**, *457*, 706.
[58] T. Yamada, Y. Hayamizu, Y. Yamamoto, Y. Yomogida, A. Izadi-Najafabadi, D. N. Futaba, K. Hata, *Nat. Nanotechnol.* **2011**, *6*, 296.
[59] X. Ho, J. N. Tey, W. Liu, C. K. Cheng, J. Wei, *J. Appl. Phys.* **2013**, *113*, 044311.
[60] F. Xu, Y. Zhu, *Adv. Mater.* **2012**, *24*, 5117.

[61] P. Lee, J. Ham, J. Lee, S. Hong, S. Han, Y. D. Suh, S. E. Lee, J. Yeo, S. S. Lee, D. Lee, S. H. Ko, *Adv. Funct. Mater.* **2014**, *24*, 5671.
[62] M.-S. Lee, K. Lee, S.-Y. Kim, H. Lee, J. Park, K.-H. Choi, H.-K. Kim, D.-G. Kim, D.-Y. Lee, S. Nam, J.-U. Park, *Nano Lett.* **2013**, *13*, 2814.
[63] M. Zu, Q. Li, G. Wang, J.-H. Byun, T.-W. Chou, *Adv. Funct. Mater.* **2013**, *23*, 789.
[64] Z. H. Jiang, Z. Cui, T. W. Yue, Y. Zhu, D. H. Werner, *IEEE Trans. Biomed. Circuits Syst.* **2017**, *11*, 920.
[65] K. Chen, Z. J. Yang, Y. J. Feng, B. Zhu, J. M. Zhao, T. Jiang, *AIP Adv.* **2015**, *5*, 067152.
[66] F. Sarrazin, S. Pflaum, C. Delaveaud, *IEEE Antennas Wireless Propag. Lett.* **2017**, *16*, 1309.
[67] L. Jelinek, M. Capek, *IEEE Trans. Antennas Propag.* **2017**, *65*, 329.
[68] J. A. Rogers, T. Someya, Y. Huang, *Science* **2010**, *327*, 1603.
[69] Y. Zhang, F. Wang, Y. Ma, X. Feng, *Int. J. Solids Struct.* **2019**, *161*, 55.
[70] Q. Zhao, Z. Liang, B. Lu, Y. Chen, Y. Ma, X. Feng, *Adv. Mater. Technol.* **2018**, *3*, 1800169.
[71] Y. H. Zhang, H. R. Fu, Y. W. Su, S. Xu, H. Y. Cheng, J. A. Fan, K. C. Hwang, J. A. Rogers, Y. G. Huang, *Acta Mater.* **2013**, *61*, 7816.
[72] Y. H. Zhang, H. R. Fu, S. Xu, J. A. Fan, K. C. Hwang, J. Q. Jiang, J. A. Rogers, Y. G. Huang, *J. Mech. Phys. Solids* **2014**, *72*, 115.
[73] Y. H. Zhang, S. D. Wang, X. T. Li, J. A. Fan, S. Xu, Y. M. Song, K. J. Choi, W. H. Yeo, W. Lee, S. N. Nazaar, B. W. Lu, L. Yin, K. C. Hwang, J. A. Rogers, Y. G. Huang, *Adv. Funct. Mater.* **2014**, *24*, 2028.
[74] R. X. Xu, J. W. Lee, T. S. Pan, S. Y. Ma, J. Y. Wang, J. H. Han, Y. J. Ma, J. A. Rogers, Y. G. Huang, *Adv. Funct. Mater.* **2017**, *27*, 1604545.
[75] V. Coskun, B. Ozdenizci, K. Ok, *Wireless Pers. Commun.* **2013**, *71*, 2259.
[76] H. U. Chung, B. H. Kim, J. Y. Lee, J. Lee, Z. Q. Xie, E. M. Ibler, K. Lee, A. Banks, J. Y. Jeong, J. Kim, C. Ogle, D. Grande, Y. Yu, H. Jang, P. Assem, D. Ryu, J. W. Kwak, M. Namkoong, J. B. Park, Y. Lee, D. H. Kim, A. Ryu, J. Jeong, K. You, B. W. Ji, Z. J. Liu, Q. Z. Huo, X. Feng, Y. J. Deng, Y. S. Xu, K. I. Jang, J. Kim, Y. H. Zhang, R. Ghaffari, C. M. Rand, M. Schau, A. Hamvas, D. E. Weese-Mayer, Y. G. Huang, S. M. Lee, C. H. Lee, N. R. Shanbhag, A. S. Paller, S. Xu, J. A. Rogers, *Science* **2019**, *363*, eaau0780.
[77] S. I. Park, D. S. Brenner, G. Shin, C. D. Morgan, B. A. Copits, H. U. Chung, M. Y. Pullen, K. N. Noh, S. Davidson, S. J. Oh, J. Yoon, K. I. Jang, V. K. Samineni, M. Norman, J. G. Grajales-Reyes, S. K. Vogt, S. S. Sundaram, K. M. Wilson, J. S. Ha, R. X. Xu, T. S. Pan, T. I. Kim, Y. G. Huang, M. C. Montana, J. P. Golden, M. R. Bruchas, R. W. Gereau, J. A. Rogers, *Nat. Biotechnol.* **2015**, *33*, 1280.
[78] K. N. Noh, S. I. Park, R. Qazi, Z. N. Zou, A. D. Mickle, J. G. Grajales-Reyes, K. I. Jang, R. W. Gereau, J. L. Xiao, J. A. Rogers, J. W. Jeong, *Small* **2018**, *14*, 1702479.
[79] S. I. Park, G. Shin, J. G. McCall, R. Al-Hasani, A. Norris, L. Xia, D. S. Brenner, K. N. Noh, S. Y. Bang, D. L. Bhatti, K. I. Jang, S. K. Kang, A. D. Mickle, G. Dussor, T. J. Price, R. W. Gereau, M. R. Bruchas, J. A. Rogers, *Proc. Natl. Acad. Sci. USA* **2016**, *113*, E8169.
[80] X. Huang, Y. H. Liu, G. W. Kong, J. H. Seo, Y. J. Ma, K. I. Jang, J. A. Fan, S. M. Mao, Q. W. Chen, D. Z. Li, H. Liu, C. X. Wang, D. Patnaik, L. M. Tian, G. A. Salvatore, X. Feng, Z. Q. Ma, Y. G. Huang, J. A. Rogers, *Microsyst. Nanoeng.* **2016**, *2*, 16052.
[81] T. Chang, Y. Tanabe, C. C. Wojcik, A. C. Barksdale, S. Doshay, Z. Y. Dong, H. Liu, M. Y. Zhang, Y. L. Chen, Y. W. Su, T. H. Lee, J. S. Ho, J. A. Fan, *Adv. Funct. Mater.* **2017**, *27*, 1703059.
[82] A. M. Hussain, F. A. Ghaffar, S. I. Park, J. A. Rogers, A. Shamim, M. M. Hussain, *Adv. Funct. Mater.* **2015**, *25*, 6565.
[83] S. Xu, Z. Yan, K. I. Jang, W. Huang, H. R. Fu, J. Kim, Z. Wei, M. Flavin, J. McCracken, R. Wang, A. Badea, Y. Liu, D. Q. Xiao, G. Y. Zhou, J. Lee, H. U. Chung, H. Y. Cheng, W. Ren, A. Banks, X. L. Li, U. Paik, R. G. Nuzzo, Y. G. Huang, Y. H. Zhang, J. A. Rogers, *Science* **2015**, *347*, 154.
[84] K.-I. Jang, K. Li, H. U. Chung, S. Xu, H. N. Jung, Y. Yang, J. W. Kwak, H. H. Jung, J. Song, C. Yang, A. Wang, Z. Liu, J. Y. Lee, B. H. Kim, J.-H. Kim, J. Lee, Y. Yu, B. J. Kim, H. Jang, K. J. Yu, J. Kim, J. W. Lee, J.-W. Jeong, Y. M. Song, Y. Huang, Y. Zhang, J. A. Rogers, *Nat. Commun.* **2017**, *8*, 15894.
[85] Y. Su, X. Ping, K. J. Yu, J. W. Lee, J. A. Fan, B. Wang, M. Li, R. Li, D. V. Harburg, Y. Huang, C. Yu, S. Mao, J. Shim, Q. Yang, P.-Y. Lee, A. Armonas, K.-J. Choi, Y. Yang, U. Paik, T. Chang, T. J. Dawidczyk, Y. Huang, S. Wang, J. A. Rogers, *Adv. Mater.* **2017**, *29*, 1604989.
[86] K. Li, X. Cheng, F. Zhu, L. Z. Li, Z. Q. Xie, H. W. Luan, Z. H. Wang, Z. Y. Ji, H. L. Wang, F. Liu, Y. G. Xue, C. Q. Jiang, X. Feng, L. M. Li, J. A. Rogers, Y. G. Huang, Y. H. Zhang, *Adv. Funct. Mater.* **2019**, *29*, 1806630.
[87] Y. Zhang, F. Zhang, Z. Yan, Q. Ma, X. Li, Y. Huang, J. A. Rogers, *Nat. Rev. Mater.* **2017**, *2*, 17019.
[88] Z. Yan, F. Zhang, F. Liu, M. Han, D. Ou, Y. Liu, Q. Lin, X. Guo, H. Fu, Z. Xie, M. Gao, Y. Huang, J. Kim, Y. Qiu, K. Nan, J. Kim, P. Gutruf, H. Luo, A. Zhao, K.-C. Hwang, Y. Huang, Y. Zhang, J. A. Rogers, *Sci. Adv.* **2016**, *2*, e1601014.
[89] B. H. Kim, F. Liu, Y. Yu, H. Jang, Z. Q. Xie, K. Li, J. Lee, J. Y. Jeong, A. Ryu, Y. Lee, D. H. Kim, X. J. Wang, K. Lee, J. Y. Lee, S. M. Won, N. Oh, J. Kim, J. Y. Kim, S. J. Jeong, K. I. Jang, S. Lee, Y. Huang, Y. H. Zhang, J. A. Rogers, *Adv. Funct. Mater.* **2018**, *28*, 1803149.
[90] F. Liu, Y. Chen, H. L. Song, F. Zhang, Z. C. Fan, Y. Liu, X. Feng, J. A. Rogers, Y. G. Huang, Y. H. Zhang, *Small* **2019**, *15*, 1804055.
[91] R. Salvado, C. Loss, R. Gonçalves, P. Pinho, *Sensors* **2012**, *12*, 15841.
[92] L. Yao, Y. Qiu, *Text. Res. J.* **2015**, *85*, 561.
[93] F. Xu, B. Wei, W. Li, J. Liu, W. Liu, Y. Qiu, *Composites, Part B* **2015**, *78*, 331.
[94] F. Xu, H. Zhu, Y. Ma, Y. Qiu, *Text. Res. J.* **2017**, *87*, 147.
[95] E. Heo, K.-Y. Choi, J. Kim, J.-H. Park, H. Lee, *Text. Res. J.* **2018**, *88*, 913.
[96] J. Lilja, P. Salonen, T. Kaija, P. d. Maagt, *IEEE Trans. Antennas Propag.* **2012**, *60*, 4130.
[97] T. Kaija, J. Lilja, P. Salonen, presented at *2010—MILCOM 2010 Military Communications Conf.*, 31 October–3 November, **2010**.
[98] M. D. Dickey, *ACS Appl. Mater. Interfaces* **2014**, *6*, 18369.
[99] M. D. Dickey, R. C. Chiechi, R. J. Larsen, E. A. Weiss, D. A. Weitz, G. M. Whitesides, *Adv. Funct. Mater.* **2008**, *18*, 1097.
[100] Y. R. Jeong, J. Kim, Z. Xie, Y. Xue, S. M. Won, G. Lee, S. W. Jin, S. Y. Hong, X. Feng, Y. Huang, J. A. Rogers, J. S. Ha, *NPG Asia Mater.* **2017**, *9*, e443.
[101] A. Qusba, A. K. RamRakhyani, J. H. So, G. J. Hayes, M. D. Dickey, G. Lazzi, *IEEE Sens. J.* **2014**, *14*, 1074.
[102] M. Wang, C. Trlica, M. R. Khan, M. D. Dickey, J. J. Adams, *J. Appl. Phys.* **2015**, *117*, 194901.
[103] A. Dey, R. Guldiken, G. Mumcu, *2013 IEEE Antennas and Propagation Society International Symposium (APSURSI)*, IEEE, Orlando, FL, USA **2013**, p. 392.
[104] M. R. Khan, G. J. Hayes, J. H. So, G. Lazzi, M. D. Dickey, *Appl. Phys. Lett.* **2011**, *99*, 161106.
[105] Y. L. Lin, C. Cooper, M. Wang, J. J. Adams, J. Genzer, M. D. Dickey, *Small* **2015**, *11*, 6397.
[106] Y. A. Huang, Y. Z. Wang, L. Xiao, H. M. Liu, W. T. Dong, Z. P. Yin, *Lab Chip* **2014**, *14*, 4205.
[107] D. Rodrigo, L. Jofre, B. A. Cetiner, *IEEE Trans. Antennas Propag.* **2012**, *60*, 1796.
[108] M. Kubo, X. F. Li, C. Kim, M. Hashimoto, B. J. Wiley, D. Ham, G. M. Whitesides, *Adv. Mater.* **2010**, *22*, 2749.

[109] B. L. Cumby, G. J. Hayes, M. D. Dickey, R. S. Justice, C. E. Tabor, J. C. Heikenfeld, *Appl. Phys. Lett.* **2012**, *101*, 174102.
[110] S. J. Mazlouman, X. J. Jiang, A. Mahanfar, C. Menon, R. G. Vaughan, *IEEE Trans. Antennas Propag.* **2011**, *59*, 4406.
[111] B. Aissa, M. Nedil, M. A. Habib, E. Haddad, W. Jamroz, D. Therriault, Y. Coulibaly, F. Rosei, *Appl. Phys. Lett.* **2013**, *103*, 063101.
[112] S. Cheng, Z. Wu, *Adv. Funct. Mater.* **2011**, *21*, 2282.
[113] S. Cheng, Z. G. Wu, P. Hallbjorner, K. Hjort, A. Rydberg, *IEEE Trans. Antennas Propag.* **2009**, *57*, 3765.
[114] M. Cosker, L. Lizzi, F. Ferrero, R. Staraj, J. M. Ribero, *IEEE Antennas Wireless Propag. Lett.* **2017**, *16*, 971.
[115] S. Cheng, A. Rydberg, K. Hjort, Z. G. Wu, *Appl. Phys. Lett.* **2009**, *94*, 3.
[116] K. Ling, K. Kim, S. Lim, *Opt. Express* **2015**, *23*, 21375.
[117] M. R. Khan, C. B. Eaker, E. F. Bowden, M. D. Dickey, *Proc. Natl. Acad. Sci. USA* **2014**, *111*, 14047.
[118] T. Rai, P. Dantes, B. Bahreyni, W. S. Kim, *IEEE Electron Device Lett.* **2013**, *34*, 544.
[119] M. S. Mannoor, H. Tao, J. D. Clayton, A. Sengupta, D. L. Kaplan, R. R. Naik, N. Verma, F. G. Omenetto, M. C. McAlpine, *Nat. Commun.* **2012**, *3*, 8.
[120] T. Inui, H. Koga, M. Nogi, N. Komoda, K. Suganuma, *Adv. Mater.* **2015**, *27*, 1112.
[121] M. Park, J. Im, M. Shin, Y. Min, J. Park, H. Cho, S. Park, M.-B. Shim, S. Jeon, D.-Y. Chung, J. Bae, J. Park, U. Jeong, K. Kim, *Nat. Nanotechnol.* **2012**, *7*, 803.
[122] Z. Li, T. R. Le, Z. Wu, Y. G. Yao, L. Y. Li, M. Tentzeris, K. S. Moon, C. P. Wong, *Adv. Funct. Mater.* **2015**, *25*, 464.
[123] B. S. Kim, J. B. Pyo, J. G. Son, G. Zi, S.-S. Lee, J. H. Park, J. Lee, *ACS Appl. Mater. Interfaces* **2017**, *9*, 10865.
[124] B. S. Kim, K. Y. Shin, J. B. Pyo, J. Lee, J. G. Son, S. S. Lee, J. H. Park, *ACS Appl. Mater. Interfaces* **2016**, *8*, 2582.
[125] L. Song, A. C. Myers, J. J. Adams, Y. Zhu, *ACS Appl. Mater. Interfaces* **2014**, *6*, 4248.
[126] R. Song, Q. Wang, B. Mao, Z. Wang, D. Tang, B. Zhang, J. Zhang, C. Liu, D. He, Z. Wu, S. Mu, *Carbon* **2018**, *130*, 164.
[127] D. Tang, Q. Wang, Z. Wang, Q. Liu, B. Zhang, D. He, Z. Wu, S. Mu, *Sci. Bull.* **2018**, *63*, 574.
[128] A. Scidà, S. Haque, E. Treossi, A. Robinson, S. Smerzi, S. Ravesi, S. Borini, V. Palermo, *Mater. Today* **2018**, *21*, 223.
[129] J. Park, J. Kim, K. Kim, S.-Y. Kim, W. H. Cheong, K. Park, J. H. Song, G. Namgoong, J. J. Kim, J. Heo, F. Bien, J.-U. Park, *Nanoscale* **2016**, *8*, 10591.
[130] Y. Zhou, Y. Bayram, F. Du, L. Dai, J. L. Volakis, *IEEE Trans. Antennas Propag.* **2010**, *58*, 2169.
[131] M. M. Mansor, S. K. A. Rahim, U. Hashim, *2014 IEEE Region 10 Symp.*, IEEE, Kuala Lumpur, Malaysia **2014**, p. 240.
[132] K. J. Vinoy, J. K. Abraham, V. K. Varadan, *IEEE Trans. Antennas Propag.* **2003**, *51*, 2296.
[133] J. S. Colburn, Y. Rahmat-Samii, *IEEE Trans. Antennas Propag.* **1999**, *47*, 1785.
[134] H. J. Sun, Z. K. Zhang, R. Q. Hu, Y. Qian, *IEEE Veh. Technol. Mag.* **2018**, *13*, 100.
[135] A. K. Skrivervik, *2013 7th Eur. Conf. on Antennas and Propagation (EuCAP)*, IEEE, Gothenburg, Sweden **2013**, p. 3627.
[136] M. A. R. Osman, M. K. A. Rahim, N. A. Samsuri, M. K. Elbasheer, M. E. Ali, *Int. J. Antennas Propag.* **2012**, *2012*, 1.
[137] S. Z. Zhu, R. Langley, *IEEE Trans. Antennas Propag.* **2009**, *57*, 926.
[138] X. Li, J. Cai, X. Lu, Y. Shi, D. Gong, D. Su, D. Zhang, *J. Mater. Chem. C* **2018**, *6*, 4191.
[139] J. Lee, P. Lee, H. Lee, D. Lee, S. S. Lee, S. H. Ko, *Nanoscale* **2012**, *4*, 6408.

